*engineering proceedings*

MDPI

*Proceeding Paper*

# Discrimination of Different Human Cell Lines by Using FT-IR Spectra Spectroscopy †

**Bahar Faramarzi [1,*], Marianna Portaccio [1], Lorenzo Manti [2,3], Maria Daniela Falco [4], Manuela Iezzi [5,6] and Maria Lepore [1]**

[1] Dipartimento di Medicina Sperimentale, Università della Campania "Luigi Vanvitelli", 80138 Napoli, Italy; marianna.portaccio@unicampania.it (M.P.); maria.lepore@unicampania.it (M.L.)
[2] Dipartimento di Fisica "E. Pancini", Università degli Studi di Napoli "Federico II", 80126 Napoli, Italy; lorenzo.manti@na.infn.it
[3] Istituto Nazionale di Fisica Nucleare—Sezione di Napoli, 80100 Napoli, Italy
[4] ASL2 Lanciano-Vasto-Chieti, UOSD di Fisica Sanitaria, 66100 Chieti, Italy; danielafalco50@gmail.com
[5] Department of Neurosciences, Imaging and Clinical Sciences, Center for Advanced Studies and Technnoogy (CAST) "G. d'Annunzio" University of Chieti-Pescara, 66100 Chieti, Italy; m.iezzi@unich.it
[6] ASL2 Lanciano-Vasto-Chieti, UOC Anatomia e Istologia Patologica, 66100 Chieti, Italy
* Correspondence: ba.faramarzi@gmail.com
† Presented at the 11th International Electronic Conference on Sensors and Applications (ECSA-11), 26–28 November 2024; Available online: https://sciforum.net/event/ecsa-11.

**Abstract:** Fourier Transform Infrared (FT-IR) spectroscopy is a powerful analytical technique to obtain molecular fingerprints of various biological samples. This study aims to compare the FT-IR spectra of three distinct cell lines, SH-SY5Y (neuroblastoma), HepG2 (hepatocellular carcinoma), and MCF-10A (epithelial mammary), to identify characteristic features in their spectra that can be used for this purpose. The FT-IR spectra revealed significant protein, lipid, and nucleic acid content variations among the cell lines. The differences mentioned above reflect each cell type's unique biochemical environment and metabolic states. This distinction can help identify different cell lines. Understanding these spectral differences can provide insights into the molecular basis of cellular functions and aid in the development of cell-specific therapeutic strategies.

**Keywords:** human cell lines; SH-SY5Y; HepG2; MCF-10A; FT-IR spectroscopy; proteins; lipids; DNA; cell identification

**Citation:** Faramarzi, B.; Portaccio, M.; Manti, L.; Falco, M.D.; Iezzi, M.; Lepore, M. Discrimination of Different Human Cell Lines by Using FT-IR Spectra Spectroscopy. *Eng. Proc.* **2024**, *6*, x. https://doi.org/10.3390/xxxxx

Academic Editor(s): Name

Published: 26 November 2024

**Copyright:** © 2024 by the authors. Submitted for possible open access publication under the terms and conditions of the Creative Commons Attribution (CC BY) license (https://creativecommons.org/licenses/by/4.0/).

## 1. Introduction

The Fourier Transform Infrared (FT-IR) spectroscopy is a powerful analytical tool used to study the molecular composition of various biological samples, including cell lines. Several studies have indicated the potential use of this technique for distinguishing between healthy and cancerous cells [1,2] and among different cell lines [3,4]. In this study, we present a comparative analysis of the FT-IR spectra of three distinct cell lines: SH-SY5Y (a human neuroblastoma cell line), MCF-10A (a non-tumorigenic human mammary epithelial cell line), and HepG2 (a human liver carcinoma cell line). SH-SY5Y, derived from a human neuroblastoma, is used for research on neuronal functions and diseases like Parkinson's. HepG2, a liver carcinoma cell line, retains many liver cell functions, making it useful in studies of liver function, toxicology, and drug metabolism. MCF-10A, a non-cancerous mammary epithelial cell line, serves as a model for normal breast cells and is valuable in breast cancer research [5–7]. The study aims to uncover molecular differences in their biochemical compositions and metabolic activities through FT-IR spectral analysis. By analyzing the spectral features of these cell lines, we aim to identify key molecular differences, which may provide insights into their biochemical composition, metabolic activities, and potential applications in biomedical research.

## 2. Materials and Methods

### *2.1. Cell Line Growth Conditions*

Three different cell lines, including SH-SY5Y (a human neuroblastoma cell line), HepG2 (a human hepatocarcinoma cell line) and MCF-10A (epithelial mammary cell line) were used in this study. The cells were grown at 37 °C in a humidified atmosphere of 95% air and 5% $CO_2$. The cell lines of SH-SY5Y and HepG2 were cultured in DMEM supplemented with 10% heat-inactivated FBS, 100 U/mL penicillin, 100 μg/mL streptomycin, and 1% L-glutamine. Cell line of MCF-10A was cultured in DMEM/F12 (Gibco 3133-028) supplemented with 5% horse serum (Gibco 26050-070), 20 ng/mL epidermal growth factor (EGF, Sigma SRP3027), 10 mg/mL insulin (Sigma I6634), 0.5 mg/mL hydrocortisone (Sigma H-0888), 100 ng/mL cholera toxin (Sigma C-8052), and antibiotics (Pen/Strep, Gibco 15070-063). The 40000 MCF-10A cells were seeded on MirrIR slides in a 6-well dish. After two days of culture and removal from the growth medium, the MirrIR slides were fixed in a 3.7% formaldehyde PBS solution for 20 min at room temperature. Subsequently, they were briefly rinsed in distilled water for 3 s to eliminate residual PBS from the cell surface. The samples were then air-dried under ambient conditions. The cell lines of SH-SY5Y and HepG2 were seeded on MirrIR slides (25 × 25 $mm^2$) (Kevley Technologies, Chesterland, OH, USA), a specific reflection FT-IR spectroscopy microscope slide, nested in Petri dish capsules. The slides were seeded at a density of about $10^4$ cells/$cm^2$ for a total of approximately 5 × $10^6$ cells/Petri.

### *2.2. FT-IR Spectroscopy Measurements*

IR absorption spectra of the cell samples were obtained using a Spectrum One FTIR (PerkinElmer, Shelton, CT, USA) spectrometer equipped with a Perkin Elmer Multiscope system infrared microscope and an MCT (mercury–cadmium–telluride) FPA (focal plane-array) detector. The measurements were performed at room temperature on cells grown on MirrIR (25 × 25 $mm^2$) slides in transflection mode. For each experimental condition, three slides were prepared. Spectra were acquired within an aperture of 100 × 100 $\mu m^2$. Different regions were investigated on every slide, and three spectra were acquired for each position. The background signal was acquired in a region of the slide free of cells. All spectra were collected using 64 scans in the range from 4000 to 600 $cm^{-1}$ with a 4 $cm^{-1}$ spectral resolution. For each FT-IR measurement the spectral ranges 1800–1000 $cm^{-1}$ (LWR) and 3600–2800 $cm^{-1}$ (HWR) were separately analyzed. LWR includes the main spectral peaks related to absorption of functional groups inside nucleic acids, lipids, proteins and carbohydrate cellular components, whereas HWR comprises spectral peaks mainly related to radiation absorption from the cellular lipid and protein components.

### *2.3. Data Analysis*

The spectra were preliminarily processed by subtracting the background signal that was acquired from a free-cell zone of the slide, and a baseline were performed on the whole data and operating a piecewise baseline correction. The spectra were then normalized using a vector normalization procedure in order to have comparable intensities adopting a Standard Normal Variate (SNV) method [8]. To evidence the spectral difference among the various cell lines difference spectra were obtained by subtracting the average SNV spectra for the different cell lines.

## 3. Results and Discussion

### *3.1. FT-IR Spectra Analysis of SH-SY5Y, HepG2, and MCF-10A Cell Lines*

Figure 1 exhibits the spectrum features of the SH-SY5Y cell line. The absorption bands observed in the SH-SY5Y spectra include amide I (1651 $cm^{-1}$) that dominant peak arising from C=O stretching vibrations, primarily associated with proteins. The amide II (1546 $cm^{-1}$), arising from N-H bending and C-N stretching vibrations. Lipid bands (2852–

2922 $cm^{-1}$) that attributed asymmetric and symmetric stretching vibrations of $CH_2$ groups. Phosphate bands (1237 $cm^{-1}$ and 1087 $cm^{-1}$), indicative of nucleic acids and phospholipids.

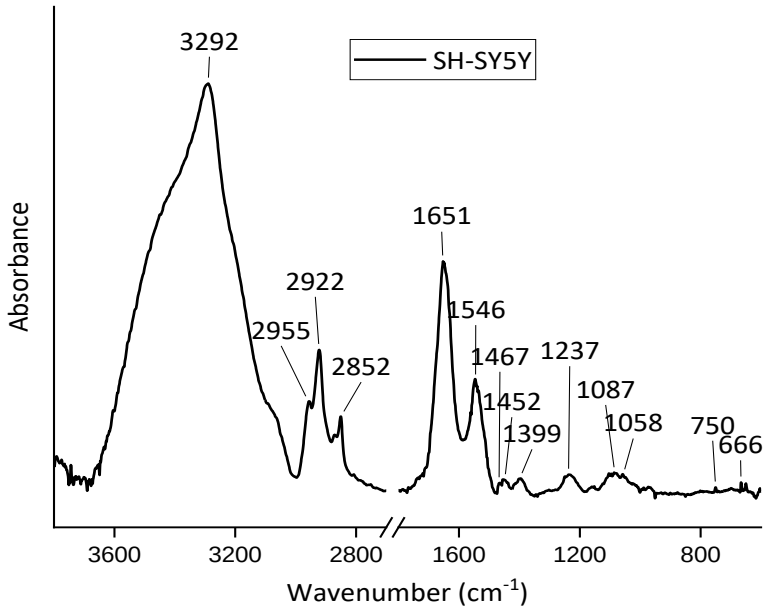


**Figure 1.** Average FT-IR spectrum obtained in transflection mode from SH−SY5Y cells.

Figure 2 displays spectral features reflecting the HepG2 cell line. Notable absorption bands include amide I and amide II bands that are similar to those seen in SH-SY5Y, but with variations in position and intensity of their peaks, suggesting differences in protein secondary structure or concentration. Prominent peaks in the 2851–2922 $cm^{-1}$ region, indicate high lipid content, typical of liver cells. In addition, peaks at 1233 and 1084 $cm^{-1}$ indicate variations in nucleic acid and phospholipid content.

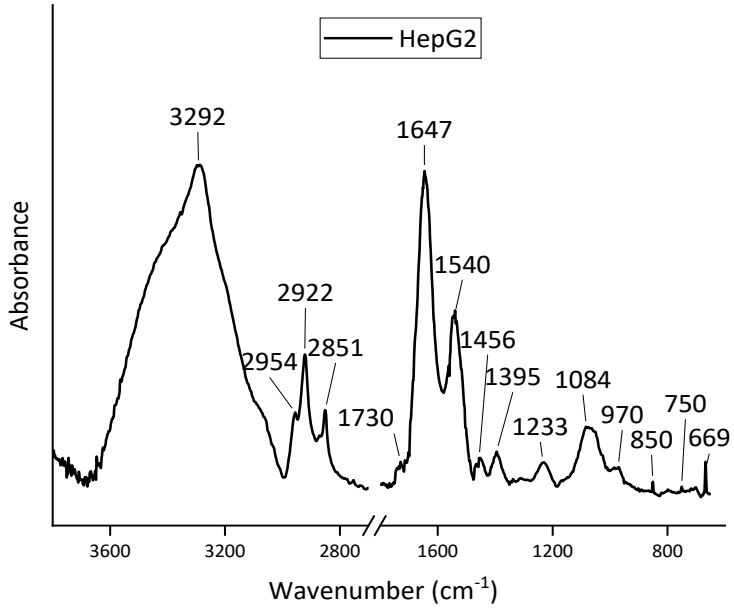


**Figure 2.** Average FT−IR spectrum obtained in transflection mode from HepG2 cells.

Figure 3 shows the spectrum features of the MCF-A10 cell line. Amide I and Amide II bands are consistent with those of SH-SY5Y and HepG2 but with different relative

intensities. Peaks in the 2850–2922 $cm^{-1}$ region, though less pronounced than in HepG2, reflect lower lipid content typical of non-cancerous cells.

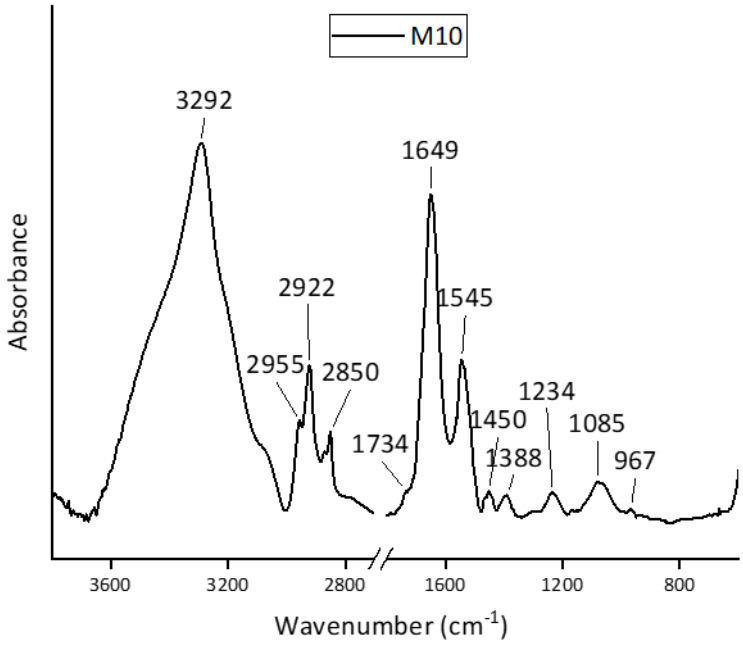


**Figure 3.** Average FT−IR spectrum obtained in transflection mode from MCF-A10 cells.

*3.2. Comparative Analysis of Cell Lines*

Table 1 presents the assignments of all major peaks in SH-SY5Y, HepG2, and MCF-10A cell lines as identified by FT-IR spectroscopy. Variations in the Amide II band suggest differences in protein secondary structures or concentrations among the three cell lines. In addition, different contributions are present only for some cell lines. See for example, the peak related C=O stretching vibration which is present in HepG2 and MCF-A10 spectra, but it is not detected in SH-AY5Y spectrum. The same occurs for other spectral features indicating difference in cell constituents.

**Table 1.** FT-IR peaks observed in the average spectrum of cell lines (SH-SY5Y, HepG2, MCF-A10), with assignments in accordance with the data reported in literature [9–11]. Abbreviation: as. = asymmetric, s. = symmetric, ν = stretching, v = vibration, δ = bending, sc.= scissoring.

| SH-SY5Y | HepG2 | MCF-A10 | Assignments | | | |
|---|---|---|---|---|---|---|
| **Peaks ($cm^{-1}$)** | **Peaks ($cm^{-1}$)** | **Peaks ($cm^{-1}$)** | **DNA/RNA** | **Protein** | **Lipids** | **Carbohydrate** |
| 3292 | 3292 | 3292 | | Amide A ($-N-H$ v) | | (O–H v) |
| 2955 | 2954 | 2955 | | $CH_3$ as. v | $CH_3$ as. v | |
| 2922 | 2922 | 2922 | | | $CH_2$ as. v | |
| 2852 | 2851 | 2850 | | | $CH_2$ s. v | |
| - | 1730 | 1734 | | (C = O s. v) | (C = O s. v) | |
| 1651 | 1647 | 1649 | | Amide I (C = O s, v) | | |
| 1546 | 1540 | 1545 | | Amide II | | |
| 1467 | - | - | | $CH_2$ δ | $CH_2$ δ | |
| - | 1456 | - | | $CH_3$ as. δ | $CH_3$ as. δ | |
| 1452 | - | 1450 | | $CH_3$ as. δ | | |
| 1399 | - | - | $CH_3$ s. δ | $CH_3$ s. δ | | |
| - | 1395 | - | | $CH_3$ s. δ | | |

| | | | | | |
|---|---|---|---|---|---|
| - | - | 1388 | | $COO^-$ s. v | $COO^-$ s. v |
| 1237 | 1233 | 1234 | $PO_2^-$ as. v | Amide III | |
| 1170 | - | - | | C– O as. v | |
| 1087 | 1084 | 1085 | $PO_2^-$ s. v | | |
| 1058 | - | - | C– O v | | |
| - | 970 | 967 | C– O s. v, $PO_2^-$ s. v | $PO_2^-$ s. v | |

*3.3. Analysis of Difference Spectra*

To highlight the modifications in the infrared spectra acquired from different cell lines, it is useful to use difference spectra. This method can reveal subtle alterations in infrared absorption features between different samples or experimental conditions [12–14]. Figures 5–7 represent the difference spectra obtained by subtracting the average SNV spectra between spectra referring to various cell lines.

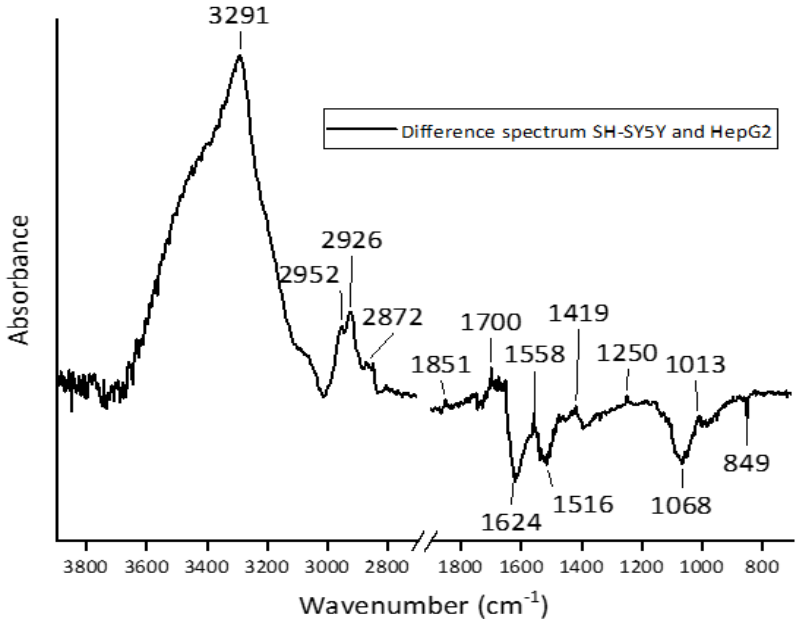


**Figure 5.** Difference spectrum of cell lines. The reported spectrum was evaluated by subtracting the mean spectrum of SH–SY5Y from the HepG2 spectrum.

Figure 5 shows the difference spectra between SH-SY5Y and HepG2, Since SH-SY5Y and HepG2 cells belong to different tissues (neuronal vs. hepatic), their protein composition and structure vary. The difference spectrum may highlight variations in the absorption or emission peaks related to proteins characteristic of each cell line, such as neural markers versus liver-specific proteins. In addition, cell membranes vary between these two cell types. HepG2 cells, being of liver origin, might show higher lipid-related absorption peaks (due to the liver's role in lipid metabolism), whereas SH-SY5Y cells may have different membrane lipid profiles. Figure 6 display the difference spectra between SH-SY5Y and MCF-A10. Differences in the position of absorption or emission peaks indicate changes in the electronic environment or molecular structure. For example, a shift in the peaks might suggest different protein folding, molecular interactions, or chromophore environments between SH-SY5Y and MCF-A10 cells.

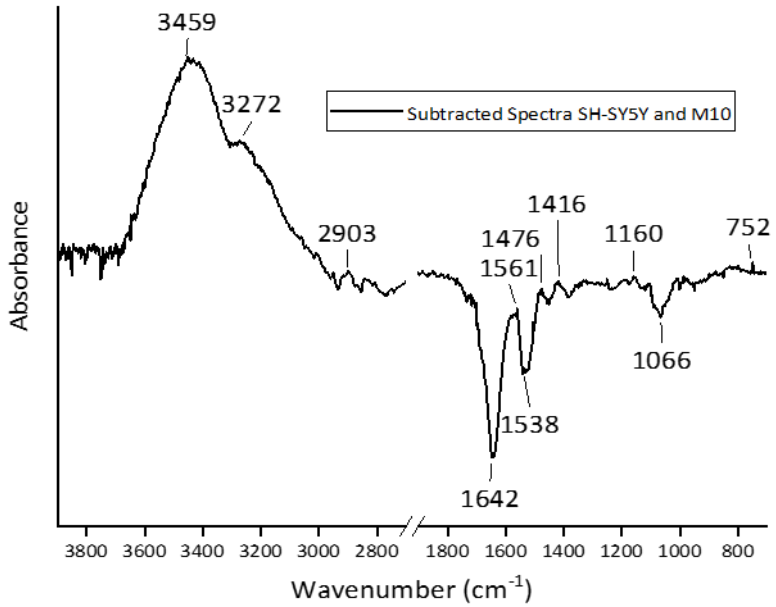


**Figure 6.** Difference spectrum of cell lines. The reported spectrum was evaluated by subtracting the mean spectrum of SH−SY5Y from the MCF−A10 spectrum.

Figure 7 evaluates difference spectrum of HepG2 and MCF-A10 cell line. Peak intensity variations could signify differences in the concentration of specific molecules, such as lipids, proteins, or nucleic acids. Since HepG2 is cancerous, it overexpresses certain proteins or metabolites compared to MCF-A10, which could lead to heightened peak intensities in certain spectral regions.

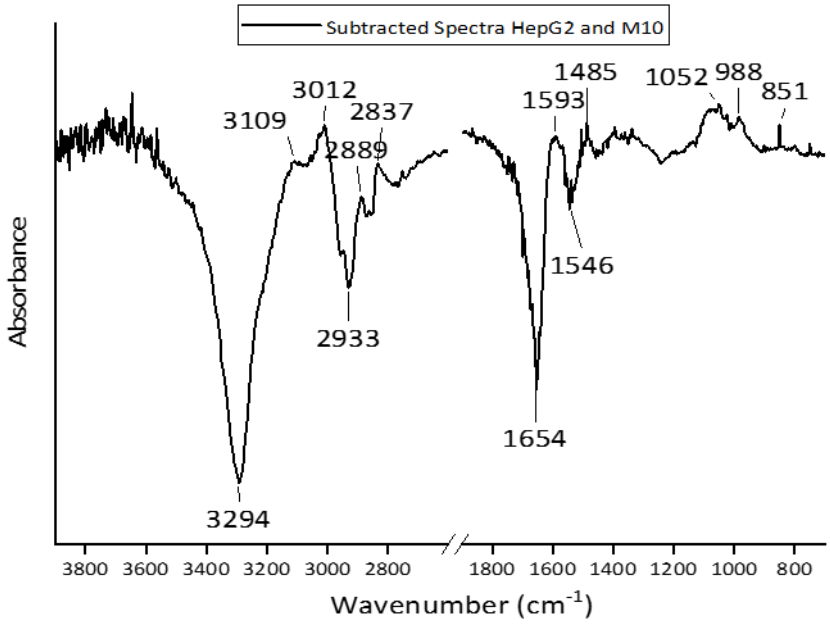


**Figure 7.** Difference spectrum of cell lines. The reported spectrum was evaluated by subtracting the mean spectrum of HepG2 from the MCF−A10 spectrum.

## 4. Conclusions

The comparative analysis of the FT-IR spectra of SH-SY5Y, MCF-10A, and HepG2 cell lines revealed significant protein, lipid, and nucleic acid content variations among the cell lines. These findings provide valuable insights into the biochemical composition and functional differences among these cell lines, highlighting the potential of FT-IR

spectroscopy in studying cellular mechanisms and disease processes in various biomedical applications. The differences mentioned above reflect each cell type's unique biochemical environment and metabolic states. This distinction can help identify different cell lines. Understanding these spectral differences can provide insights into the molecular basis of cellular functions and aid in the development of cell-specific therapeutic strategies.

**Author Contributions:** Conceptualization, M.L. and M.P.; methodology, M.P. and B.F.; software, B.F.; investigation, B.F. and M.L.; and M.P.; data curation, B.F.; writing—original draft preparation, B.F. and M.L.; writing—review and editing. B.F. and M.L. All authors have read and agreed to the published version of the manuscript.

**Funding:** This research received no external funding.

**Institutional Review Board Statement:**

**Informed Consent Statement:**

**Data Availability Statement:** Data is available on request.

**Conflicts of Interest:** The authors declare no conflict of interest.

## References

1. Lasalvia, M.; Capozzi, V.; Perna, G. Classification of healthy and cancerous colon cells by Fourier transform infrared spectroscopy. *Spectrochim. Acta Part A Mol. Biomol. Spectrosc.* **2024**, *321*, 124683.
2. Elshemey, W.M.; Ismail, A.M.; Elbialy, N.S. Molecular-level characterization of normal, benign, and malignant breast tissues using FTIR spectroscopy. *J. Med. Biol. Eng.* **2016**, *36*, 369–378.
3. Zendehdel, R.; Shirazi, F.H. Discrimination of human cell lines by infrared spectroscopy and mathematical modeling. *Iran. J. Pharm. Res. IJPR* **2015**, *14*, 803.
4. Wang, Y.; Dai, W.; Liu, Z.; Liu, J.; Cheng, J.; Li, Y.; Li, X.; Hu, J.; Lü, J. Single-cell infrared microspectroscopy quantifies dynamic heterogeneity of mesenchymal stem cells during adipogenic differentiation. *Anal. Chem.* **2020**, *93*, 671–676.
5. Xie, H.-R.; Hu, L.-S.; Li, G.-Y. SH-SY5Y human neuroblastoma cell line: In vitrocell model of dopaminergic neurons in Parkinson's disease. *Chin. Med. J.* **2010**, *123*, 1086–1092.
6. López-Terrada, D.; Cheung, S.W.; Finegold, M.J.; Knowles, B.B. Hep G2 is a hepatoblastoma-derived cell line. *Hum. Pathol.* **2009**, *40*, 1512.
7. Vale, N.; Silva, S.; Duarte, D.; Crista, D.M.; da Silva, L.P.; da Silva, J.C.E. Normal breast epithelial MCF-10A cells to evaluate the safety of carbon dots. *RSC Med. Chem.* **2021**, *12*, 245–253.
8. Lasch, P. Spectral pre-processing for biomedical vibrational spectroscopy and microspectroscopic imaging. *Chemom. Intell. Lab. Syst.* **2012**, *117*, 100–114.
9. Talari, A.C.S.; Martinez, M.A.G.; Movasaghi, Z.; Rehman, S.; Rehman, I.U. Advances in Fourier transform infrared (FTIR) spectroscopy of biological tissues. *Appl. Spectrosc. Rev.* **2017**, *52*, 456–506.
10. Ricciardi, V.; Portaccio, M.; Piccolella, S.; Manti, L.; Pacifico, S.; Lepore, M. Study of SH-SY5Y cancer cell response to treatment with polyphenol extracts using FT-IR spectroscopy. *Biosensors* **2017**, *7*, 57.
11. Movasaghi, Z.; Rehman, S.; ur Rehman, D.I. Fourier transform infrared (FTIR) spectroscopy of biological tissues. *Appl. Spectrosc. Rev.* **2008**, *43*, 134–179.
12. Gasper, R.; Dewelle, J.; Kiss, R.; Mijatovic, T.; Goormaghtigh, E. IR spectroscopy as a new tool for evidencing antitumor drug signatures. *Biochim. Biophys. Acta (BBA)-Biomembr.* **2009**, *1788*, 1263–1270.
13. Delfino, I.; Ricciardi, V.; Manti, L.; Lasalvia, M.; Lepore, M. Multivariate analysis of difference raman spectra of the irradiated nucleus and cytoplasm region of SH-SY5Y human neuroblastoma cells. *Sensors* **2019**, *19*, 3971.
14. Lorenz-Fonfria, V.A. Infrared difference spectroscopy of proteins: From bands to bonds. *Chem. Rev.* **2020**, *120*, 3466–3576.

**Disclaimer/Publisher's Note:** The statements, opinions and data contained in all publications are solely those of the individual author(s) and contributor(s) and not of MDPI and/or the editor(s). MDPI and/or the editor(s) disclaim responsibility for any injury to people or property resulting from any ideas, methods, instructions or products referred to in the content.